A first-passage-time theory for search and capture of chromosomes by microtubules in mitosis

Manoj Gopalakrishnan* and Bindu S. Govindan†

Department of Physics, Indian Institute of Technology (Madras), Chennai 600036, India

(Dated: October 22, 2018)

Abstract

The mitotic spindle is an important intermediate structure in eukaryotic cell division, in which each of a pair of duplicated chromosomes is attached through microtubules to centrosomal bodies located close to the two poles of the dividing cell. Several mechanisms are at work towards the formation of the spindle, one of which is the 'capture' of chromosome pairs, held together by kinetochores, by randomly searching microtubules. Although the entire cell cycle can be up to 24 hours long, the mitotic phase typically takes only less than an hour. How does the cell keep the duration of mitosis within this limit? Previous theoretical studies have suggested that the chromosome search and capture is optimized by tuning the microtubule dynamic parameters to minimize the search time. In this paper, we examine this conjecture. We compute the mean search time for a single target by microtubules from a single nucleating site, using a systematic and rigorous theoretical approach, for arbitrary kinetic parameters. The result is extended to multiple targets and nucleating sites by physical arguments. Estimates of mitotic time scales are then obtained for different cells using experimental data. In yeast and mammalian cells, the observed changes in microtubule kinetics between interphase and mitosis are beneficial in reducing the search time. In *Xenopus* extracts, by contrast, the opposite effect is observed, in agreement with the current understanding that large cells use additional mechanisms to regulate the duration of the mitotic phase.

* manoj@physics.iitm.ac.in

† bindu@physics.iitm.ac.in

Key words: microtubule, chromosome capture, metaphase spindle, Green's functions

I. INTRODUCTION

Microtubules are one class of polymeric filaments in the eukaryotic cell, whose sub-unit is a hetero-dimer of alpha- and beta-tubulin. Microtubules therefore possess structural polarity, and the ends are differentiated as plus and minus ends. A hall-mark of microtubules is their unique mechanism of assembly and dis-assembly: a polymerizing microtubule can abruptly start shrinking by losing sub-units and *vice-versa*, a process referred to as dynamic instability(reviewed in [1]). The stochastic switching process between growth and shrinkage is referred to as catastrophe and the reverse process is called rescue. Between a rescue and a catastrophe, a microtubule grows in length by polymerizing and between a catastrophe and rescue, it shrinks. In vivo, a third state called pause is also observed where the length remains static. Microtubules usually nucleate from organizing centers called centrosomes, but may also be found free in the cytoplasm.

Microtubules play a central role in eukaryotic cell division. An important milestone in the cell division cycle is the formation of the metaphase spindle, where all the duplicated chromosome pairs, held together by kinetochores are aligned along the cell 'equator (the "metaphase plate") in such a way that each chromosome of a pair is facing one of the poles of the cell, and attached to one or more microtubules emanating from a centrosome located near that pole. The spindle starts forming when microtubules nucleating from each centrosome randomly searches the surrounding space for chromosomes by alternately growing and shrinking (the random search-and-capture model, and are stabilized upon contact with a kinetochore[2, 3]. Investigations over the last decade or so have revealed that the chromosomes do not always remain passive in this process; rather, the kinetochores nucleate and stabilize microtubules in their vicinity, a process facilitated by RanGTP, which then connect to the astral microtubules emanating from the chromosomes, assisted by motor proteins such as dynein (see [4] for a recent review). In the present paper, we, however, restrict ourselves to the situation where chromosomes are passive, and microtubules perform the search-and-capture.

We now briefly review the previous papers that addressed this problem. A theoretical and numerical study of the random search-and-capture model was done first by Holy and

Leibler[5]. In this paper, the conditions for optimization of search process was investigated for a spherical cell of radius $R = 50\mu$m, with a single stationary target at various distances $d < R$ from the centre. The number of searching polymers was fixed at 250, and was assumed to remain constant with time (effectively infinite nucleation rate). At the cell boundary, the filaments would stop growing and wait until a catastrophe occurs. By a combination of intuitive arguments and explicit simulations, it was postulated that (i) the global minimum of the search time occurs when rescue is absent and (ii) the optimized mean time of search increases with d, and is less than 10 minutes for $d < 10\mu$m, but much higher for larger d. In a more recent paper, Wollman et al[6] carried out a more detailed study of the problem, and also investigated the time to capture multiple chromosomes. An optimal catastrophe frequency was first estimated by minimizing a weighted average time of search for multiple chromosomes at variable separations from the nucleating centre. Numerical simulations of the problem, using this optimal frequency showed that the search typically took hours to complete when the number of targets was large (eg. 46 in humans). However, when a biochemically induced bias in search (a microtubule stabilizing RanGTP gradient around chromosomes) was introduced, the search was completed over physiologically reasonable times.

In the earlier studies, it has generally been assumed, on the basis of probabilistic arguments, that the rescue frequency should be optimally zero. However, small, but non-zero rescue frequency is typically observed in mitotic cells, and the existing theoretical results cannot be used to analyze this case. Also, the earlier studies have generally ignored the finite cell size which limits long searches, and is likely to be crucial at least in small cells. The number of searching microtubules was generally assumed constant, while this is a fluctuating quantity, controlled by the nucleation rate at the centrosomes.

The primary motivation behind the present paper is to present a rigorous theoretical method for calculating the search time for arbitrary rescue frequency, nucleation rate and cell size/radius. The formalism presented here is based on a set of Greens functions and first passage densities for microtubule dynamics, related through a set of convolution equations. As such, this approach permits us to derive an implicit expression for the probability distribution of the search time for a single chromosome/target. Existing theoretical results follow from our more general expressions in the appropriate limits.We believe that this formalism will be useful in obtaining a great deal of insight into microtubule dynamics in *in*

vivo situations, and may well find applications in other related problems.

In the following sections, we discuss the problem and the model, develop the formalism to address the problem, and analyze our results, first in theoretically interesting limits. The results are then discussed in the context of available experimental observations. We then conclude with a summary of our findings and mention a few directions in which this study may be extended. Two appendices supplement the mathematical part of the paper.

II. MATHEMATICAL FORMALISM

A. Model details

It is convenient to imagine that during pro-metaphase, prior to division, the shape of the cell is close to an ellipsoid. Microtubules nucleate from two centrosomes, which, for simplicity, may be assumed to be located at the two focal points of the ellipsoid, and the duplicated chromosomes, held together through kinetochores (henceforth called simply 'targets') are assumed to be scattered around the equatorial plane. In the rest of this paper, we only consider capture of the target by microtubules emanating from one of the centrosomes, which is a precursor event to the later 'bi-oriented' configuration, where microtubules from both centrosomes will bind to a target and engage in 'tug-of-war' which ultimately separates the individual chromosomes in the pair.

It is generally estimated that there are hundreds of nucleating sites in a centrosome. From a vacant site, a microtubules nucleate at rate ν in a random direction and grows by polymerization as long as it is in the growth phase, while the same microtubule shrinks in length by depolymerization in the shrinking phase. Catastrophe and rescue frequencies are denoted by ν_c and ν_r respectively, and are assumed to be the same everywhere inside the cell, as are the growth and shrinkage velocities, denoted v_g and v_s. In this paper, as in the earlier papers which addressed this problem, we will treat all these different dynamical quantities are independent parameters (see the discussion in the last section, however). In the process, the microtubule scans the surrounding space for chromosomes, and is stabilized when the growing end encounters a kinetochore.

A microtubule from a certain nucleation site on the centrosome can nucleate in many possible directions; however, given the finite size of the centrosome, the orientation is likely

to be constrained by the geometry of the centrosome. In an extreme case, one **may** imagine that a microtubule will always grow only along the local normal to the surface, but this case is pathological when the target is fixed in space, since no microtubule might ever grow in the right direction to find it. It is therefore, more realistic to imagine that microtubules from each nucleation site in the centrosome will grow within a certain solid angle $\Delta\Omega$, which defines a *search cone* for the corresponding nucleation site. In this case, if the fixed target falls inside the cone, and has a cross-sectional area a, it subtends a solid angle a/d^2 at a point on the centrosome, and therefore a microtubule originating at that particular site has a probability $p = ad^{-2}\Delta\Omega^{-1}$ for nucleating in the *right* direction, within the search cone of the site.

For a given search process, $\Delta\Omega$ is determined by several factors, the most important being (a) orientational constraints on nucleation at a given site in the centrosome and (b) steric hindrance between microtubules in the cytoplasm. In general, one may see that when $\Delta\Omega$ is large, p is small, and consequently, the search by microtubules from any single nucleating site becomes inefficient. However, in this case, the search cones of different microtubules overlap (each being large) and more nucleating sites/microtubules will be able to participate in the search.On the other hand, if $\Delta\Omega$ is small, only a few microtubules will be effectively searching, however the search by each is now more efficient; the two effects therefore compensate each other. For concreteness, we choose $\Delta\Omega = \pi/2$ in this paper, i.e., a microtubule from any nucleating site will be able to search a quarter of the space around it (This choice is somewhat arbitrary and not directly derived from any experimental data; for comparison, Wollman et. al[6] used $\Delta\Omega = 2\pi$). An illustration of the model is shown in Fig.1. We take the cross-sectional area of a target to be $a = 0.25\mu\text{m}^2$ throughout this paper (corresponding to a radius of $\sim 0.28\mu$m), therefore, with the previous estimate of $\Delta\Omega$, we find $p \simeq 0.31/d^2$, where d is measured in μm.For $d = 2\mu$m and larger, therefore $p \ll 1$.

A search by microtubules emanating from any particular site is terminated in three possible ways: if the nucleation occurs in the right direction, (i) the growing tip encounters the target and ends the search, or (ii) the microtubule depolymerizes completely before it encounters the target, and finally (iii) if the nucleation happens in the wrong direction, the microtubule will ultimately depolymerize and disappear after a futile search, with or without encountering the cell boundary. For mathematical simplicity, we assume that within a search cone, the boundary is at the same distance R from the centre, although this is strictly true

only when $\Delta\Omega$ is sufficiently small. The cut-off distance R therefore serves as an estimate of the size of the cell. In the last case, we assume that once the microtubule hits the cell boundary, it undergoes catastrophe at a rate ν_c', which is generally higher than the value in the interior [7–9]. In particular, it was reported in [7] that the catastrophe frequency near the boundary is 16-fold higher than that in the interior, for certain cells. In cases (ii) and (iii), a new microtubule will nucleate again from the center in a randomly chosen direction, at rate ν.

Search cones of many nucleating sites will overlap, and therefore a target will be searched simultaneously by many microtubules which will reduce the mean search time. It was shown in Wollman et. al[6] that the mean time to capture N targets by M microtubules (M nucleating sites in our case) is given by

$$T_{M,N} \simeq T_{1,1}\frac{\sigma_N}{M} \tag{1}$$

where $\sigma_N = \sum_{k=1}^{N} k^{-1} \sim \log N$ when $N \gg 1$.The above expression holds, provided the probability distribution of the search for a single target by a single microtubule is a pure exponential (which is true only for zero rescue frequency, as in [6], but not true in general). Further, Eq.1 is true only if all the targets are at the same distance from the centrosome/microtubule nucleating centre, which is not true in a realistic situation. When the targets are at variable separations, an estimate of the mean search time can be still obtained in the form of the following inequality:

$$T_{M,N} < T_{1,1}^{\max}\frac{\sigma_N}{M} \tag{2}$$

where $T_{1,1}^{\max}$ is the search time for the farthest target, which is an upper limit on $T_{1,1}$. In this paper, we compute $T_{1,1}$ rigorously, with some simplifying assumptions, but for arbitrary kinetic parameters. We then use Eq.2 to make estimates for multiple targets and parallel search, for the sake of comparison with experiments.

B. Capture time distribution

For the rest of this paper, we replace $T_{1,1}$ simply by T. Let us denote by $C(T)$ the probability density of the capture time T for a single stationary target at a certain distance from the centrosome. The mean capture time follows:

$$\langle T \rangle = \frac{\int_0^\infty dTC(T)T}{\int_0^\infty dTC(T)}, \tag{3}$$

where, $\int_0^\infty dTC(T)$ is the probability that the search will be eventually successful, which we will, later, show to be unity.

Since the basic process under consideration here is the capture of a certain target by one (or a set) of dynamically unstable filaments, it is natural to base our theory on consideration of first passage probability densities[10, 11]. For this purpose, it is convenient to define a set of three *conditional* first passage probability densities (CFPD), which will serve as the basic quantities in terms of which the probability distribution $C(T)$ can be expressed. These CFPDs are defined below, with the corresponding condition for each given in italics.

1. $K_1(T) \equiv p\Phi(d,T)$, where $\Phi(d,T)$ is the CFPD for a freshly nucleated microtubule to reach a distance d for the first time after a time interval T, *without ever shrinking back to the origin in between.*

2. $K_2(T) \equiv (1-p)Q_R(T)$, where $Q_X(T)$ is the CFPD for shrinking to the origin after a life-time T, *without ever reaching a length X in between.*

3. $K_3(T) \equiv (1-p)\Psi(T)$, where $\Psi(T)$ is the CFPD for return to the origin after a time interval T, *after encounter with the boundary (and consequent catastrophe) at least once (and possibly several times) in between.*

A successful search event is, in general, preceded by n unsuccessful search events: let us denote by $\Omega_n(T)$ the probability of n unsuccessful nucleation-search-disappearance events within a time interval T, so that $C(T)$ may be written as

$$C(T) = \sum_{n=0}^{\infty} \int_0^T \Omega_n(T-T')p\Phi(d,T')\nu dT' \tag{4}$$

Our next task is to write an expression for $\Omega_n(T)$. Let us now assume that among the n unsuccessful nucleation events, there are n_1 events of type 1 (above), where the microtubule nucleated in the right direction, but did not reach the chromosome, n_2 events of type 2 (above), where it nucleated in a wrong direction, but shrank back to origin before encountering the boundary, and $n_3 = n - n_1 - n_2$ events of type 3 (above), where the microtubule

nucleated in a wrong direction, encountered the boundary, underwent catastrophe and then shrank to the origin.

Specifying the total number of events in each class does not completely describe the history of the process, as the temporal ordering of the events is still arbitrary. The n_1 events of type 1 can be distributed in a total of n in $\binom{n}{n_1}$ different ways, and the n_2 events of type 2 can be distributed among the remaining $n - n_1$ in $\binom{n-n_1}{n_2}$ different ways. The remaining $n - n_1 - n_2$ events naturally belong to type 3.

$\Omega_n(T)$ may now be expressed as a sum over histories (i.e., a *path-integral*) of all these events, ordered temporally in all possible ways. This is done as follows: Starting at time $T = 0$, let the first microtubule nucleation occur at time T_1', and let this microtubule live for a time interval T_1. Then there is a time gap of T_2' until the next nucleation, and the microtubule nucleated then lasts for a time interval T_2 and so on. The time gap T_1' occurs with a probability $\exp(-\nu T_1')$ and the nucleation at the end of it occurs with probability $\nu dT_1'$. The probability that a microtubule will last for a time interval T_1 before shrinking back to the origin may be denoted $K(T_1)dT_1$, but K could be K_1, K_2 or K_3 depending on whether this event falls into type 1, 2 or 3. For $\Omega_n(T)$, there are a total of n such nucleation-death events within a time interval T. The resulting mathematical expression can be written as a convolution over all these time-intervals, and has the form

$$\Omega_n(T) = \sum_{n_1=0}^{n} \sum_{n_2=0}^{n-n_1} \sum_{per} \int_0^T \nu dT_1' e^{-\nu T_1'} \int_0^{T-T_1'} dT_1 K(T_1) ..... \int_0^{T-T_1'-..T_{n-1}} dT_n K(T_n) e^{-\nu[T-\sum_{k=1}^{n}(T_k+T_k')]} \tag{5}$$

where *per* stands for all the possible permutations of events, as far as their temporal order of occurrence is concerned. The preceding equation has the form of a $2n$-fold convolution, and it is therefore convenient to use Laplace transforms. We define $\tilde{\Omega}_n(s) = \int_0^\infty dT e^{-sT} \Omega_n(T)$ and similarly for other quantities. A generalized form of the standard convolution theorem for Laplace transforms may be applied to Eq.5 (see, eg.,[12]), and the result is

$$\tilde{\Omega}_n(s) = \frac{1}{(s+\nu)} \left(\frac{\nu}{s+\nu} \right)^n \sum_{n_1=0}^{n} \sum_{n_2=0}^{n-n_1} \binom{n}{n_1} \binom{n-n_1}{n_2} \tilde{K}_1(s)^{n_1} \tilde{K}_2(s)^{n_2} \tilde{K}_3(s)^{n-n_1-n_2} \tag{6}$$

Note that, in the passage from Eq.5 to Eq.6, allowance has been made for the fact that the random variable K takes the value K_1 n_1 times, K_2 n_2 times and K_3 $n - n_1 - n_2$ times. The previous equation is clearly a binomial series, and can be summed immediately. From Eq.4, we find $\tilde{C}(s) = \nu p \tilde{\Phi}(d,s) \sum_{n=0}^{\infty} \tilde{\Omega}_n(s)$. After substituting the binomial sum from Eq.6, and replacing K_1, K_2, K_3 by their original notations, we arrive at the following expression:

$$\tilde{C}(s) = \frac{\nu p \tilde{\Phi}(d,s)}{\left[s + \nu \left(1 - p\tilde{Q}_d(s) - (1-p)[\tilde{Q}_R(s) + \tilde{\Psi}(s)] \right) \right]} \tag{7}$$

As a special case, if MT nucleation occurs very fast and therefore not rate-limiting, we may take the limit $\nu \to \infty$ in the above equation, whence the following limiting form is reached:

$$\lim_{\nu \to \infty} \tilde{C}(s) = \frac{p \tilde{\Phi}(d,s)}{1 - \left[p\tilde{Q}_d(s) + (1-p) \left(\tilde{Q}_R(s) + \tilde{\Psi}(s) \right) \right]} \tag{8}$$

Eq.7 is the central result of this paper. Using this expression, the mean search time for a single target, and its variance may be expressed as

$$\langle T \rangle = -\frac{\partial_s \tilde{C}(s)|_{s=0}}{\tilde{C}(0)} \quad ; \quad \langle T^2 \rangle = \frac{1}{\tilde{C}(0)} \frac{\partial^2 \tilde{C}(s)}{\partial s^2}|_{s=0}, \tag{9}$$

where $\tilde{C}(0) = \int dT C(T)$. It is, however clear that $\tilde{\Phi}(d,0) + \tilde{Q}(d,0) = 1$, since a microtubule growing in the right direction will either have to hit the target, or shrink back without touching the target. Similarly, for the wrong directions, we have the relation $\tilde{Q}(R,0) + \tilde{\Psi}(0) = 1$ for similar reasons. Substitution of these normalization relations into Eq.7 shows that $\tilde{C}(0) = 1$ for all parameters, i.e., the search is always eventually successful.

The CFPDs introduced above are now calculated from the Green's functions for MT kinetics, derived explicitly in the next section.

C. Green's functions

The stochastic state of a MT at a given point in time t is characterized by two variables, its length l and its state of polymerization versus depolymerization, which we denote by an index i,which takes one of the two values,1 or 0 respectively for growing and shrinking states. In this case, therefore, we need to compute four Green's functions, or propagators,

$G_{ij}(x,t;x_0,0)$, for $i,j = 0,1$; by definition, $G_{ij}(x,t;x_0,0)dx$ gives the probability that a given MT will have length l between x and $x+dx$, and will be in state i at time t, provided that it had a length x_0 and was at state j at an earlier time $t = 0$.

Calculating the above Green's functions for a physically realistic situation would also require specification of appropriate boundary conditions at the origin (nucleating site) and this has been done earlier[13]. However, we deem this unnecessary for our purpose, since we are only interested in using these Green's functions to compute the CFPDs introduced above. Therefore, for the rest of this paper, we will allow the 'length' x to be a continuously varying variable between positive and negative values, with no boundary condition imposed on the dynamics at $x = 0$. The boundary conditions are used in the definition of the CFPDs later.

The Dogterom-Leibler[14] rate equations for MT kinetics takes the form

$$\begin{aligned} \partial_t G_{1j} &= -v_g \partial_x G_{1j} + \nu_r G_{0j} - \nu_c G_{1j} \\ \partial_t G_{0j} &= v_s \partial_x G_{0j} + \nu_c G_{1j} - \nu_r G_{0j} \end{aligned} \tag{10}$$

The equations may be solved together using combined Laplace-Fourier transforms, defined as $\tilde{G}_{ij}(k,s;x_0) = \int_{-\infty}^{\infty} e^{-ikx} dx \int_0^{\infty} dt e^{-st} G_{ij}(x,t;x_0,0)$. The solution is

$$\tilde{G}_{ij}(k,s) = \frac{e^{-ikx_0}[\nu_r - \delta_{ij}(ikv_s - s)]}{v_s v_g [k^2 - ikA(s) + B(s)]} \tag{11}$$

where

$$\begin{aligned} A(s) &= [v_s \nu_c - v_g \nu_r + s(v_s - v_g)]/v_s v_g \\ B(s) &= [s(s + \nu_r + \nu_c)]/v_s v_g. \end{aligned} \tag{12}$$

For connection with the **CFPD**s introduced earlier, it is convenient to define the Green's function in such a way as that they have dimensions of inverse time, and not inverse length. This is done by defining

$$F_{1j} = v_g G_{1j} \quad ; \quad F_{0j} = v_s G_{0j} \tag{13}$$

It will be convenient for later calculations to carry out the inversion $k \to x$ explicitly:

$$\tilde{F}_{1j}(x,s;x_0) = \frac{\nu_r + s\delta_{1j}}{v_s[\alpha_s+\beta_s]}\left[e^{-\alpha_s(x-x_0)}\Theta(x-x_0) + e^{\beta_s(x-x_0)}\Theta(x_0-x)\right] + \frac{\delta_{1j}}{(\alpha_s+\beta_s)}\left[\alpha_s e^{-\alpha_s(x-x_0)}\Theta(x-x_0) - \beta_s e^{\beta_s(x-x_0)}\Theta(x_0-x)\right]$$
$$\tilde{F}_{0j}(x,s;x_0) = \frac{\nu_c + s\delta_{0j}}{v_g[\alpha_s+\beta_s]}\left[e^{-\alpha_s(x-x_0)}\Theta(x-x_0) + e^{\beta_s(x-x_0)}\Theta(x_0-x)\right] - \frac{\delta_{0j}}{(\alpha_s+\beta_s)}\left[\alpha_s e^{-\alpha_s(x-x_0)}\Theta(x-x_0) - \beta_s e^{\beta_s(x-x_0)}\Theta(x_0-x)\right] \tag{14}$$

where

$$\alpha_s = \frac{A(s)}{2} + \sqrt{B(s) + A^2(s)/4}$$
$$\beta_s = -\frac{A(s)}{2} + \sqrt{B(s) + A^2(s)/4} \tag{15}$$

and $\Theta(x)$ is the usual step-function: $\Theta(x) = 1$ for $x \geq 0$ and 0 otherwise.

D. Calculation of $\Phi(d,T)$ and $Q_X(T)$

The Green's functions calculated in the last section may now be used to compute the CFPDs which we used before. For this purpose, it is convenient to define first a set of *unconditional* first passage densities (denoted FPD) as follows: let $C_{ij}(x,t;x_0,0)$ denote the probability, per unit time, for a MT in state j and with length x_0 at time $t=0$, to reach a length x for the first time at time t, and in state i.

For $l > 0$, $C_{11}(l,t;0,0)$ is given by the implicit equation

$$F_{11}(l,t;0,0) = C_{11}(l,t;0,0) + \lim_{\epsilon\to 0+}\int_0^t dt' C_{11}(l,t';0,0)F_{11}(l-\epsilon,t;l,t') \tag{16}$$

In the above equation (and the following equations), the ϵ-factors take into account the following restriction on its dynamics: starting from a growing state at $t=0$, with a length l, it can return to the same length l at a later time, in a growing state, only from below (which decides which of the Θ-functions appearing in Eq.14 is non-zero). Similar restrictions apply to the equations below.

Similarly, $C_{01}(0,T;d,0)$ and $C_{10}(d,T;0,0)$ are given by the equations

$$F_{01}(0,T;d,0) = C_{01}(0,T;d,0) + \lim_{\epsilon\to 0+}\int_0^T dT' C_{01}(0,T';d,0)F_{00}(\epsilon,T;0,T') \tag{17}$$

$$F_{10}(d,T;0,0) = C_{10}(d,T;0,0) + \lim_{\epsilon\to 0+}\int_0^T dT' C_{10}(d,T';0,0)F_{11}(d-\epsilon,T;d,T') \tag{18}$$

Using these two FPDs, we are now in a position to write down the following relations between the CFPDs introduced earlier:

$$C_{11}(d,t;0,0) = \Phi(d,t) + \int_0^t dt' Q_d(0,t')C_{10}(d,t;0,t') \tag{19}$$

$$C_{01}(0,T;0,0) = Q_d(T) + \int_0^T dT' \Phi(d,T')C_{01}(0,T;d,T') \tag{20}$$

Eq.16-20 may now be solved using Laplace transforms. From Eq.16, we find that

$$\tilde{C}_{11}(d,s;0) = \lim_{\epsilon\to 0+}\frac{\tilde{F}_{11}(d,s;0)}{1+\tilde{F}_{11}(d-\epsilon,s;d)} = e^{-\alpha_s d} \tag{21}$$

Similarly,

$$\tilde{C}_{10}(d,s;0) = \frac{\nu_r e^{-\alpha_s d}}{\nu_r + s + \alpha_s v_s} \quad ; \quad \tilde{C}_{01}(0,s;d) = \frac{\nu_c e^{-\beta_s d}}{\nu_c + s + \beta_s v_g} \tag{22}$$

After solving Eq.19 and Eq.20 together, and using Eq.21,22, we find the explicit expressions

$$\tilde{\Phi}(d,s) = \frac{D(s)e^{-\alpha_s d}}{\nu_r\nu_c[1-e^{-(\alpha_s+\beta_s)d}] + D(s)}$$
$$\tilde{Q}_d(s) = \frac{\nu_c}{\nu_c + s + \beta v_g}\left[1 - e^{-\beta_s d}\tilde{\Phi}(d,s)\right] \tag{23}$$

where

$$D(s) = (s+\alpha_s v_s)(s+\beta_s v_g) + \nu_r(s+\beta_s v_g) + \nu_c(s+\alpha_s v_s). \tag{24}$$

E. Calculation of $\Psi(T)$: Catastrophes at the cell boundary

We assume that when a MT hits the cell boundary by growing, it undergoes catastrophe there at a rate ν_c'. We now compute $\Psi(T)$, which is the CFPD of return to origin (i.e., complete depolymerization) of a MT after a lifetime T, and an encounter with the boundary at least once.

Clearly, along the line of our previous arguments, $\Psi(T)$ may be given by the expression

$$\Psi(T) = \int_0^T dT_1 \Phi(R, T_1) \times \int_0^{T-T_1} \nu_c' dT_2 e^{-\nu_c' T_2} \chi(R, T - T_1 - T_2), \tag{25}$$

where $\chi(R, T)$ gives the FPD of complete depolymerization of a MT, starting at the boundary, at length R in shrinking state, with possibly multiple visits back to the boundary in between. This quantity may now be expressed implicitly through the equation

$$\chi(R, T) = \Phi^*(R, T) + \int_0^T dT_1 Q_R^*(T_1) \times \int_0^{T-T_1} \nu_c' dT_2 e^{-\nu_c' T_2} \chi(R, T - T_1 - T_2) \tag{26}$$

where $Q_R^*(T)$ is a 'mirror' image, or *dynamic inverse* of the quantity $Q_R(T)$ introduced earlier, and represents the CPFD of a return to boundary over a time interval T, without ever reaching the origin (i.e., shrinking to zero) in between. Similarly, $\Phi^*(R, T)$ is the 'inverse' of $\Phi(R, T)$, and gives the CFPD of complete depolymerization of a MT starting at the boundary, without ever returning to the boundary in between.

Eq.25 and Eq.26 may now be solved together using Laplace transforms, and we find

$$\tilde{\Psi}(s) = \frac{\nu_c' \tilde{\Phi}(R, s) \tilde{\Phi}^*(R, s)}{s + \nu_c' \left(1 - \tilde{Q}_R^*(s)\right)} \tag{27}$$

The inverse quantities $\tilde{\Phi}^*(R, s)$ and $\tilde{Q}_R^*(s)$ may be obtained from $\tilde{\Phi}(R, s)$ and $Q_R(s)$ respectively by the transformations $v_s \leftrightarrow v_g$ and $\nu_r \leftrightarrow \nu_c$. From Eq.15, this has the effect of replacing α_s by β_s and *vice-versa*, while $D(s)$ defined in Eq.24 remains invariant under

these transformations. Therefore, using Eq.23, we arrive at the following expressions for these 'inverse' quantities:

$$\tilde{Q}^*_R(s) = \frac{\nu_r}{\nu_r + s + \alpha_s v_s}\left[1 - e^{-\alpha_s R}\tilde{\Phi}^*(R,s)\right] \tag{28}$$

$$\tilde{\Phi}^*(R,s) = \frac{D(s)e^{-\beta_s R}}{\nu_r\nu_c[1 - e^{-(\alpha_s+\beta_s)R}] + D(s)} \tag{29}$$

Eq.29 completes the list of quantities that we need to compute the mean search time. We now start from Eq.9, and after a few elementary calculations and rearrangement of terms, it turns out that the complete expression for the mean search time may be written out as follows(see Appendix A for details):

$$\langle T\rangle = N_s[pt_d + (1-p)t_R + t_\nu] = T_d + \frac{1-p}{p}T_R + T_\nu \tag{30}$$

where $N_s = [p\tilde{\Phi}_d(0)]^{-1}$ gives the mean number of unsuccessful search events before each successful one, and $pt_d + (1-p)t_R + t_\nu$ gives the weighted mean lifetime per event. $t_d = -\tilde{\Phi}'_d(0) - \tilde{Q}'(d,0)$ gives the mean time of a search in the right direction, the first term corresponding to the single successful search event and the second giving the mean of all unsuccessful events. $t_R = -\tilde{Q}'_R(0) - \tilde{\psi}'(0)$ is the mean lifetime of an unsuccessful search event in the wrong direction, the first term corresponding to events not reaching the boundary while the second corresponds to events which hit the boundary at least once. Note that t_R is the mean lifetime of microtubules. Finally, $t_\nu = \nu^{-1}$ is the mean time between the disappearance of one microtubule and nucleation of a new one at a site, and is the only term that depends on the nucleation rate ν.

Various quantities such as the mean, standard deviation and higher moments (if necessary) of the search time, as well as other quantities such as the mean lifetime of microtubules may now be calculated using the set of equations presented in this section, and parameters such as catastrophe and rescue frequencies as well as growth and shortening velocities taken from experiments. We found it convenient to use Mathematica (Version 7, Wolfram Research) to carry out the explicit computations. The results will be discussed in the following section.

III. RESULTS

In this section, we will analyze some experimental observations using the results from our model.Experimental measurements of the microtubule kinetic parameters show that distinct changes occur as the cell progresses from interphase to mitosis[15], see Table I. Budding Yeast cells show a reduction in both catastrophe and rescue frequencies, but the changes are relatively small. In mammalian cells, which are typically larger, there is a marked fall in rescue frequency between interphase and mitosis, and a two-fold increase in catastrophe frequency. In *Xenopus* oocytes (frog egg cells, which are large and almost 1 mm in radius), the effects are somewhat different: the rescue frequency, while small, is almost doubled, but more remarkably, there is a sharp, seven-fold rise in the catastrophe frequency.

Given that mitosis occupies only a small fraction of the total time duration of a cell cycle, we first seek to determine whether the changes in microtubule kinetics are beneficial to reduce the mean time of search. For all cases discussed below, we choose $\nu_c' = 10\nu_c$ to be roughly consistent with experiments[7]. However, reducing or increasing ν_c' by an order of magnitude does not significantly affect the results.

A. Yeast and mammalian cells show features that are consistent with the random search and capture model, but *Xenopus* oocytes do not

Fig.2 shows a comparison for the mean time of search, between interphase and mitosis values in yeast, for a range of target distance d. Since yeast undergoes closed mitosis, the relevant boundary cut-off length scale is the nuclear radius, which we take to be $R = 2\mu$m. The mitosis parameters clearly reduces the time scale relative to the interphase parameters, though understandably, given the small cut-off radius of search, the effect is small. When the centrosomal microtubule nucleation frequency is chosen to be $\nu = 0.1\text{min}^{-1}$ per site (see next paragraph) $\langle T \rangle$ in yeast is found to vary from 100-400 minutes, for d between 1μm and 2μm. Taking $T_{1,1}^{\max} \sim 400$ min, and using $N = 32$ in budding yeast, we see from Eq.2 that the mean time to complete search is 24 min, with 50 searching microtubules.

We now turn to the case of mammalian cells. Experiments by Piehl et. al[16] measured a nucleation rate of $\sim$ 80-100 min^{-1}, per centrosome in kidney epithelial (LLCPK) cells. The total number of nucleation sites is unknown, but from the measured surface area of

centrosomes in metaphase ($\sim 100\ \mu\text{m}^2$), and the base area of a single microtubule ($\pi r^2 \simeq 4 \times 10^{-4} \mu\text{m}^2$, with $2r = 25nm$), a total of almost 10^5 nucleation sites are possible, which is clearly too large; as a conservative estimate, we may assume a total of 1000 nucleation sites. Then, the nucleation rate per site may be roughly estimated as $\nu \simeq 0.1\text{min}^{-1}$.

Let us now perform our analysis on a mammalian cell of radius $R = 20\mu$m, and compare the search time between interphase and mitosis. As seen in Fig.3, where the logarithm of the time is shown against the distance d, the mitosis values significantly reduce the mean search time, almost by 4 orders of magnitude! For $d = 6\mu$m, the time computed from mitosis values is $T_{1,1}^{\max} \simeq 2000$ minutes. If we conservatively assume that at least $M = 100$ kinetochore microtubules will be actively searching for one target, and since $N > 10$ typically (46 in humans), using Eq.2, we arrive at an estimate of 35-40 minutes for the total mean search time, which is reasonable. However, this is only the average time, and may not represent a typical value. We have observed that the standard deviation of T is typically of the same order as $\langle T \rangle$; therefore, in an individual experiment, the search could take twice as long.

In *Xenopus* extracts, the situation is very different (see Fig.4). In this case, surprisingly, it is the interphase parameter values that give the lower mean search time, and mitosis time is typically 1-2 orders of magnitude larger! Even the interphase mean search time is quite large, ranging from 2000-10,000 minutes for d between 5 and 10 μm, and it would need almost 1000 actively searching microtubules to bring the total search time down to acceptable values. The anomalously large value of the catastrophe frequency in mitosis is puzzling, since targets that are far are more effectively searched when ν_c is small. . How do we understand this discrepancy? One reason, as is now becoming increasingly clear, could be that the random search and capture mechanism is simply inefficient in such large cells. Indeed, it is now well-established that large cells like oocytes require additional mechanisms of search like actin contractile ring[17] and guided search through RanGTP gradient around chromosomes[6, 18]. In the latter case, microtubules are preferentially stabilized close to chromosomes hy a gradient of the protein Ran, and the increased catastrophe frequency might simply serve to enhance the turnover rate, and hence the dynamicity of microtubules.

B. Mathematical analysis show that $\nu_r = 0$ is a minimum condition when $R \gg d$

In this section, we take a closer look at the theoretical expression for the mean search time derived earlier, and try to understand some general features, from the point of view of optimization of the search process, i.e., minimization of the search time. Without any loss of generality, we may put $\nu = \infty$ here, as the only effect of a finite ν is to add a timescale of ν^{-1} to the mean time (see Eq.30).

It is instructive to look at the mean search time separately for parameter regimes demarcated by the conditions $A(0) > 0$ and $A(0) < 0$. Physically, these conditions correspond to a bounded growth regime for the filaments, with finite mean length and unbounded growth regime with mean length linearly increasing with time[14]. After rather lengthy algebraic calculations, an explicit expression for $\langle T \rangle$ can be obtained, and the terms therein could be classified into two: (i) those that remain finite, or diverge as $R \to \infty$ and (ii) those that involve only terms of the form $e^{-R|A(0)|}$ which disappear for large R. In the following, we ignore terms that fall into (ii), since they are not crucial for our analysis here.

Bounded growth regime (BG); $A(0) > 0$:

In this case, $\tilde{\Phi}(d,0) = D_0 e^{-A(0)d}/[D_0 + \nu_r \nu_c (1 - e^{-A(0)d})]$, so that the mean number of trials N_s diverges exponentially with d. The breakup of the total time in the limit $R|A(0)| \to \infty$, is as below:

$$T_d = \frac{\beta' + v_g^{-1}}{A(0)}[e^{A(0)d} - 1] - \beta' d$$
$$T_R \simeq \left(1 - \frac{\nu_r v_g}{\nu_c v_s} e^{-A(0)d}\right) \frac{e^{A(0)d} \nu_c v_s (v_s + v_g)}{(v_s v_g A(0))^2} \tag{31}$$

where $\beta' = (\nu_r + \nu_c)/v_s v_g A(0)$. In this regime, T_d and T_R diverge exponentially with d, but only linearly with R, with the R-dependence entirely disappearing for $R \gg A(0)^{-1}$ (terms now shown in the equation). This is physically reasonable, since $A(0)^{-1}$ is indeed the mean length of the filaments in this regime. We also observe that T_R diverges as $A(0)^{-2}$ and T_d diverges as $A(0)^{-1}$ as $A(0) \to 0$. The intuitive explanation is that, at this 'critical point' in parameter space, the tip of a microtubule performs a pure one-dimensional random walk, whose mean time of return to the origin is infinite, as is well-known.

The $R|A(0)| \gg 1$ limit, with some further simplifications, is treated in more detail in Appendix B. We will now give the corresponding results for the case $A(0) < 0$.

Unbounded growth regime(UBG): $A(0) < 0$:

In this case, $\tilde{\Phi}(d,0) = D_0/(D_0 + \nu_r\nu_c[1 - e^{-|A(0)|d}]$, which is finite as $d \to \infty$. This is natural, because under conditions of unbounded growth, the microtubules are able to reach out to larger distances with fewer attempts compared to the bounded growth regime. Similar to the previous case, we may now calculate the breakup of the terms in the limit $R|A(0)| \gg 1$ and $\nu_c' \to \infty$. The results are given below:

$$\begin{aligned} T_d &= \frac{|A(0)|}{\nu_r v_g}F(d) - \frac{\nu_c v_s}{\nu_r v_g}\beta' d + \frac{\nu_c(v_s - v_g)}{v_g^2 v_s |A(0)|^2}[1 - e^{-|A(0)|d}] \\ T_R &\simeq \frac{\nu_r v_g}{H(d)}\left\{\frac{v_s}{\nu_r}|A(0)|F(R) + F^*(R) - \frac{\nu_c v_s}{\nu_r v_g}\beta' R + \frac{\nu_c(v_s - v_g)}{v_g^2 v_s |A(0)|^2} + \right. \\ &\qquad \left. \frac{v_g + v_s}{v_g v_s |A(0)|}\left[e^{|A(0)|R}\left(1 + \frac{\nu_r}{v_s|A(0)|}\right) - 1\right]\right\} \end{aligned} \tag{32}$$

where

$$\begin{aligned} H(d) &= \nu_c v_s - \nu_r v_g e^{-|A(0|d} \\ F(R) &= -\frac{D'}{D_0} + \frac{D'}{D_0 + \nu_r\nu_c} + \alpha' R \\ F^*(R) &= F(R) + (\beta' - \alpha')R \\ \alpha' = \frac{\nu_r + \nu_c}{v_g v_s |A(0)|} \quad &; \quad \beta' = \frac{v_s^2\nu_c - v_g^2\nu_r}{(v_s v_g)^2 |A(0)|} \end{aligned} \tag{33}$$

In contrast to the previous case, T_R diverges exponentially with R, while T_d diverges only linearly with d. As $|A(0)| \to 0$, the mean time again diverges as $|A(0)|^{-2}$ as before. The exponential divergence with R arises solely from the boundary-interaction term $\tilde{\Psi}'(0)$; the return-to-origin term $\tilde{Q}'(0)$ has a finite limit as $R \to \infty$.This result is in quantitative agreement with the corresponding results in [13] for the mean time of return to origin of a microtubule in unbounded (as well as bounded) growth phase.

The analogy between the dynamics of the tip of a microtubule and a one-dimensional biased random walk as developed in [13] is helpful in understanding these results. It has been shown that the bias (drift) of this random walk is proportional to $v_g\nu_r - v_s\nu_c$, i.e., the bias is negative when (in our notation) $A(0) > 0$ ('bounded growth phase'), positive when $A(0) < 0$ ('unbounded growth phase') and the walk is unbiased (i.e., the tip moves diffusively) when $A(0) = 0$. In the limit $R \to \infty$, T_R and T_d diverge as $A(0) \to 0$ simply

because the mean time of return to origin of a one-dimensional random walk is infinite, whereas this time is finite for a biased random walk.

We may now make a few general observations from these results. For a single target, as considered here, it is appropriate to assume that $p \ll 1$, in which case, the T_R term dominates over T_d in Eq.30. If $R \gg d$, the exponential divergence of T_R with R in the UBG regime makes it less favourable compared to the bounded growth regime. For the latter case, at least when $R \gg A(0)^{-1}$, it is proved in Appendix B that T_R is a monotonically increasing function of ν_r, i.e., it is minimized for $\nu_r = 0$. Therefore, we conclude that if the cell boundary is sufficiently far in comparison with d, for a single target, search is optimal if the microtubules are in a bounded growth phase, at zero rescue frequency. This conclusion is in agreement with the previous authors[5, 6].Interestingly, these conclusions hold even if R is only about thrice as large as d, as shown in Fig.5, or even when $d = R$ (Fig.6).

In a more realistic situation where a number of chromosomes are distributed randomly in the cytoplasm at varying distances, p itself effectively becomes a dynamic variable, starting at a large value and progressively decreasing with time as targets are captured one by one. In this situation, it is likely that search is optimized at a small, but non-zero rescue frequency. Preliminary results shown in Fig.6 suggest that when the target is far from the centrosome, non-zero rescue does not increase the mean search time significantly, and in addition, could produce a more robust minimum.

C. Non-zero rescue is likely to be a compromise between $\nu_r = 0$ and $\nu \to \infty$

If the search time is minimized at zero rescue frequency, as shown by the previous arguments, why is not the observed rescue frequency in mitosis *even smaller*? We believe that this could possibly reflect a compromise between minimizing rescue and maximizing nucleation. Both rescue frequency and nucleation rate depend directly on the concentration of free tubulin in cytoplasm. Experimental observations by Walker et. al.[19] have shown that rescue frequency is an almost linearly increasing function of free GTP-tubulin concentration, and nucleation rate is an even more strongly increasing function of concentration. Therefore, the observed rescue frequency in mitosis could probably be understood as the result of a more general optimization exercise also involving nucleation and catastrophe frequencies, as well as growth velocity, all of which depend on free GTP-tubulin concentration.

D. Microtubule turnover time is much smaller in mitosis

In Fig.7A, we show the mean lifetime (defined in Eq.30) of microtubules searching in the wrong directions, as a function of cell size R, in both interphase and mitosis. The lifetime in mitosis is several orders of magnitude smaller than interphase, and varies little with cell size (a direct consequence of being in the BG regime discussed earlier). However, mitotic microtubules are also more dynamic: the standard deviation of the lifetime as a fraction of the mean, is larger in mitosis compared to interphase (Fig.7B). Experimental observations in mammalian cells have shown that microtubule turnover in mitosis is 18-fold higher than in interphase[20].

IV. CONCLUSIONS

In this paper, we studied the capture of a target by dynamically unstable microtubules using a novel and mathematically rigorous first passage time-based formalism. Compared to earlier studies, the principal new features in our model are (a) estimation of the mean time of capture at non-zero rescue frequency (b) introduction of the cell size as a parameter in the theory and (c) explicit comparison with experimental observations in different mitotic cells. Although the model was formulated for the purpose of understanding chromosome capture in mitosis, the formalism itself is very general. In particular, the technique could be directly applied to the study of cortical capture of microtubules(see, eg.[23]) and other similar problems.

Several *in vivo* experiments have shown distinct and significant changes in microtubules dynamics in different cells, as the cell proceeds from interphase to mitosis. We sought to determine whether these changes are beneficial to the search and capture of chromosomes. Our analysis shows that in yeast and mammalian cells, the mean search time for a single target is reduced in mitosis compared to interphase. In *Xenopus* oocytes, by contrast, the experimental observations could not be reconciled with the observed changes in microtubule dynamics between interphase and mitosis, suggesting that the basic strategy of search may be strongly modified by additional mechanisms.

Although this was not our main interest, we also tried to determine theoretically the conditions for minimization of the mean search time. We showed rigorously that when the

target is well inside the boundary, the time is minimized at zero rescue and an optimal catastrophe frequency, in agreement with previous authors. However,when the target is close to the boundary, although $\nu_r = 0$ is still the absolute minimum, it was observed that a small, but non-zero ν_r produced a more robust minimum (with respect to change in ν_c), and therefore could be preferred by cells.

The present study was only concerned with a single target, while in all realistic situations, multiple chromosome pairs have to be captured. Unfortunately, to extend the present analysis to multiple targets would require more detailed knowledge of $C(T)$, but given the complexity of the mathematical form for $\tilde{C}(s)$, this is not too easy(see, however, [6], where this analysis was done for exponentially decaying $C(T)$ at $\nu_r = 0$). We are presently working on extracting information about $C(T)$ from our formalism, and extending our analysis for multiple targets. In particular, it is not immediately clear whether the optimization criteria for multiple targets will be the same as for a single target, especially when multiple targets are at variable separations from the centrosome. Further, as discussed earlier, the various dynamic parameters for microtubule dynamics are not generally independent (eg. nucleation and rescue could be related, and detailed GTP cap theories suggest that growth velocity is related to catastrophe frequency[24]). A more general optimization scheme has to take these possibilities into account, and could produce a non-zero optimal rescue frequency. We leave these ideas to a future study.

Other possible extensions of this study involve including (i) chromosome diffusion (ii) side-capture of microtubules by chromosomes through intermediaries like kinesin-13 motor proteins, followed by one-dimensional diffusive or directed motion to the tip[25] and (iii) microtubule nucleation close to the chromosomes. The latter is a possible alternative to the end-capture mechanism studied in this paper and it would be interesting to look at its effect on the mitotic time-scales and its optimization.

ACKNOWLEDGMENTS

BG acknowledges financial support under a Young Scientist-Fast Track Research Fellowship, from the Department of Science and Technology, Government of India. MG would like to thank Mohan Balasubramanian (NUS, Singapore) for a brief but illuminating conversation on mitosis in yeast. MG's work was supported in part by a grant from the Centre

for Industrial Consultancy and Sponsored Research, IIT Madras. The authors are thankful for the hospitality under the Visitors Program at the Max-Planck Institute for Physics of Complex Systems, Dresden, Germany, where this work was initiated.

---

[1] Desai A and Mitchison T J (1997) Microtubule polymerization dynamics *Annu. Rev. Cell. Dev. Biol.* **13** 83.

[2] Kirschner M and Mitchison T J (1986) Beyond self-assembly: From microtubules to morphogenesis *Cell* **45** 329

[3] Hayde J H, Bowser S S and Reider C L (1990) Kinetochores capture astral microtubules during chromosome attachment to the mitotic spindle: direct visualization in live newt lung cells *J. Cell. Biol.* **111** 1039

[4] O'Connell C B and Khodjakov A L (2007) Cooperative mechanisms of mitotic spindle formation *J. Cell. Sci.* **120** 1717

[5] Holy T E and Leibler S (1994) Dynamic instability of microtubules as an efficient way to search in space *Proc. Natl. Acad. Sci. USA* **91** 5682

[6] Wollman R, Cytrynbaum E N, Jones J T, Meyer T, Scholey J M and Mogilner A (2005) Efficient chromosome capture requires a bias in the 'Search-and-Capture' process during mitotic-spindle assembly *Curr. Biol.* **15** 828

[7] Komarova Y A, Vorobjev I A and Borisy G G (2002) Life cycle of MTs: persistent growth in the cell interior, asymmetric transition frequencies and effects of the cell boundary *J. Cell. Sci.* **115**(17) 3527

[8] Govindan B S and Spillman W B, Jr. (2004) Novel steady state of a microtubule assembly in a confined geometry *Phys. Rev. E Stat. Nonlin. Soft Matter Phys.* **70** 032901

[9] Gregoretti I V, Margolin G, Alber M S and Goodson H V(2006) Insights into cytoskeletal behavior from computational modeling of dynamic microtubules in a cell-like environment *J. Cell Sci.* **119** 4781

[10] Van Kampen N G (1992) *Stochastic processes in Physics and Chemistry* (North Holland).

[11] Redner S (2001) *A guide to First-Passage Processes* (Cambridge University Press).

[12] M. Gopalakrishnan, P. Borowski, F. Jülicher and M. Zapotocky (2007) Response and fluctuations of a two-state signaling module with feedback *Phys. Rev. E. Stat. Nonlin. Soft Matter*

Phys. **76** 021904.

[13] Bicout D J (1997) Green's functions and first passage time distributions for dynamic instability of microtubules *Phys. Rev. E. Stat. Nonlin. Soft Matter Phys.* **56** 6656.

[14] Dogterom M and Leibler S (1993) Physical aspects of growth and regulation of microtubule structures *Phys. Rev. Lett.* **70**(9) 1347.

[15] Rusan N M, Fagerstrom C J, Yvon, A C and Wadsworth P (2001) Cell cycle-dependent changes in microtubule dynamics in living cells expressing green fluroscent protein-α tubulin *Mol. Biol. Cell* **12** 971.

[16] Piehl M, Tulu U S, Wadsworth P and Cassimeris L (2004) Centrosome maturation: Measurement of microtubule nucleation throughout the cell cycle by using GFP-tagged EB1 *Proc. Natl. Acad. Sci. USA* **101**(6) 1584.

[17] Lenart P, Bacher C P, Daigle N, Hand A R, Eils R, Terasaki M and Ellenberg J (2005) A contractile nuclear actin network drives chromosome congression in oocytes *Nature* **436** 812.

[18] Ohba T, Nakamura M, Nishitani H, and Nishimoto T (1999) Self-organization of microtubule asters induced in Xenopus egg extracts by GTP-bound Ran. *Science* **284** 1356.

[19] Walker R A, O'Brien E T, Pryer N K, Sobeiro M F, Voter W A, Erickson H P and Salmon E D (1988) Dynamic instability of individual microtubules analyzed by video light microscopy: rate constants and transition frequencies *J. Cell. Biol.* **107** 1437.

[20] Saxton W M, Stemple D L, Leslie R J,Salmon E D, Zavortink M and McIntosh J R (1984) Tubulin dynamics in cultured mammalian cells *J. Cell. Biol.* **99** 2175.

[21] Tirnauer J S, O'Toole E, Berrueta L, Bierer B E and Pellman D (1999) Yeast Bim1p promotes the G1-specific dynamics of microtubules *J. Cell. Biol.* **145**(5) 993.

[22] Belmont L D, Hyman A A, Sawin K E and Mitchison T J (1990) Real-time visualization of cell cycle dependent changes in microtubule dynamics in cytoplasmic extracts *Cell* **62** 579.

[23] Lee L, Tirnauer JS, Li J, Schuyler SC, Liu JY and Pellman D (2000) Positioning of the mitotic spindle by a cortical-microtubule capture mechanism *Science* **287** 2260.

[24] Flyvbjerg H, Holy T E and Leibler S (1996) Microtubule dynamics: Caps, catastrophes, and coupled hydrolysis *Phys. Rev. E.Stat. Nonlin. Soft Matter Phys.* **54** 5538.

[25] Howard J. and Hyman A A (2007) Microtubule polymerases and depolymerases *Curr. Opin. Cell. Biol.* **19** 31.

V. APPENDIX I

General expression for the mean search time:

After a series of calculations, the following general expression is reached for the mean search time from Eq.7.

$$\langle T\rangle = T_d + \frac{1-p}{p}T_R + \frac{1}{p}T_\nu \tag{34}$$

with

$$\begin{aligned} T_d &= -[\tilde{\Phi}(d,0)]^{-1}\left[\tilde{\Phi}'(d,0) + \tilde{Q}'(d,0)\right] \\ T_R &= -[\tilde{\Phi}(d,0)]^{-1}\left[\tilde{Q}'(R,0) + \tilde{\Psi}'(0)\right] \\ T_\nu &= \frac{1}{\nu}[\tilde{\Phi}(d,0)]^{-1} \end{aligned} \tag{35}$$

where $\tilde{\Phi}'(d,0) = \partial_s\tilde{\Phi}(d,s)|_{s=0}$, $\tilde{Q}'(d,0) = \partial_s\tilde{Q}(d,s)|_{s=0}$,$\tilde{Q}'(R,0) = \partial_s\tilde{Q}(R,s)|_{s=0}$ and $\tilde{\Psi}'(0) = \partial_s\tilde{\Psi}(s)|_{s=0}$. Here, T_d, T_R and T_ν represent, respectively, the mean time spent in searching in the right direction, wrong directions and between successive nucleations.We note that the last term disappears in the (theoretical) $\nu \to \infty$ limit, where the nucleation happens infinitely fast. Also, for small p, T_R and T_ν dominate over T_d, since, in this limit, it is the unsuccessful search events that take up most of the time spent on search.

The exact analytical forms for these functions are as given below:

$$\begin{aligned} \tilde{\Phi}'(X,0) &= \tilde{\Phi}(X,0)\left[\frac{D'}{D_0} - \frac{D' + \nu_r\nu_c(\alpha'+\beta')Xe^{-\gamma_0 X}}{D_0 + \nu_r\nu_c(1-e^{-\gamma_0 X})} - \alpha' X\right] \\ \tilde{Q}'(X,0) &= -\tilde{Q}(X,0)\left[\frac{1+\beta' v_g}{\nu_c + \beta_0 v_g} + e^{-\beta_0 X}\frac{[\tilde{\Phi}'(X,0) - \beta' X\tilde{\Phi}(X,0)]}{[1-\tilde{\Phi}(X,0)e^{-\beta_0 X}]}\right] \\ \tilde{\Psi}'(0) &= \tilde{\Psi}(0)\left[\frac{\tilde{\Phi}'(R,0)}{\tilde{\Phi}(R,0)} + \frac{\tilde{\Phi}^{*\prime}(R,0)}{\tilde{\Phi}^*(R,0)} - \frac{[1-\nu_c'\tilde{Q}^{*\prime}(R,0)]}{\nu_c'[1-\tilde{Q}^*(R,0)]}\right] \end{aligned} \tag{36}$$

and

$$\begin{aligned} \tilde{\Phi}^{*\prime}(R,0) &= \tilde{\Phi}'(R,0; v_g \to v_s, \nu_r \to \nu_c) \\ \tilde{Q}^{*\prime}(R,0) &= \tilde{Q}'(R,0; v_g \to v_s, \nu_r \to \nu_c) \end{aligned} \tag{37}$$

are the mirror-image quantities defined in text. The time-integrated probabilities $\tilde{\Phi}(d,0), \tilde{Q}(X,0)(X=d,R)$ and $\tilde{\Psi}(0)$ are given by

$$\begin{aligned}\tilde{\Phi}(X,0) &= \frac{D_0 e^{-\alpha_0 X}}{D_0 + \nu_r \nu_c [1 - e^{-\gamma_0 X}]} \\ \tilde{Q}(X,0) &= \frac{\nu_c}{\nu_c + \beta_0 v_g} \left[1 - \tilde{\Phi}(X,0) e^{-\beta_0 X}\right] \\ \tilde{\Psi}(0) &= \frac{\tilde{\Phi}(R,0)\tilde{\Phi}^*(R,0)}{1 - \tilde{Q}^*(R,0)}. \end{aligned} \tag{38}$$

The cofficients appearing in the above expressions are defined as follows:

$$\begin{aligned}\alpha_0 \equiv \alpha(0); \alpha' &= \partial_s \alpha(s)|_{s=0} \\ \beta_0 \equiv \beta(0); \beta' &= \partial_s \beta(s)|_{s=0} \\ D_0 \equiv D(0); D' &= \partial_s D(s)|_{s=0} \end{aligned} \tag{39}$$

and $\theta = \partial_s A(s)|_{s=0} = (v_s - v_g)/v_s v_g$, $\theta' = \partial_s B(s)|_{s=0} = (\nu_r + \nu_c)/v_s v_g$.

VI. APPENDIX II

Some simple special cases in BG regime

If $p \ll 1$, T_R and T_ν dominate over T_d, and, from Eq.30 and Eq.31 we have

$$\langle T \rangle \simeq \frac{e^{A(0)d}}{p} \left(1 + \frac{\nu_r (1 - e^{-A(0)d})}{v_s A(0)}\right) \left[\frac{v_s + v_g}{v_s v_g A(0)} + \frac{1}{\nu}\right] \qquad (p \ll 1, R \to \infty) \tag{40}$$

It can be shown that this expression is a monotonically increasing function of ν_r, where $0 \leq \nu_r < (v_g/v_s)\nu_c$ in the BG regime. In order to see this, let us define $x = \nu_c v_s$ and $y = \nu_r v_g$, and $x - y > 0$ in this regime. Then, in terms of x and y, the mean search time may be expressed in the form

$$\langle T \rangle_{x,y} = \frac{[x e^{\delta(x-y)} - y]}{(x-y)} \left[\frac{a_1}{(x-y)} + b_1\right] \geq \frac{a_1}{(x-y)} + b_1 \tag{41}$$

where a_1, b_1 and δ are positive constants, and the inequality follows because $e^{\delta(x-y)} \geq 1$. The lower bound in the above equation continuously increases with y in the applicable range [0:x]. We then conclude that $\langle T \rangle$ itself is an increasing function of y, and hence ν_r. Therefore, $\nu_r = 0$ is a necessary condition for a minimum. In this case, Eq.40 reduces to

$$\langle T \rangle = \left[\frac{1}{\nu} + \frac{1}{\nu_c}(1 + v_g/v_s) \right] \frac{e^{\frac{\nu_c d}{v_g}}}{p} - \frac{d}{v_s} \quad (p \ll 1, R \to \infty, \nu_r = 0) \tag{42}$$

which is minimized $\nu_c = \nu_c^{\min}$, where

$$\nu_c^{\min} = \frac{2v_g}{d\left[1 + \sqrt{1 + \frac{4v_g}{d\nu(1+v_g/v_s)}}\right]} \quad (p \ll 1, R \to \infty, \nu_r = 0) \tag{43}$$

Finally, in the limit $\nu \to \infty$, $\nu_c^{\min} = v_g/d$, and the optimized search time is

$$\langle T \rangle^{\min} = \Gamma d^3 - \frac{d}{v_s}; \quad (p \ll 1, R \to \infty, \nu_r = 0, \nu \to \infty) \tag{44}$$

where $\Gamma = e\Delta\Omega/[a(v_g^{-1} + v_s^{-1})]$ from Eq.1.

The expression in Eq.42 above may be approximately reproduced by physical arguments as follows[5]. The probability that a microtubule will nucleate in the right direction, and will not undergo catastrophe until it reaches the target is given by $p_s = pe^{-\nu_c d/v_g}$, and it will take at least $N \sim p_s^{-1}$ unsuccessful attempts before this is accomplished. Each of these unsuccessful search events lasts a time $\tau \sim \nu_c^{-1}$, and therefore, the total search time is

$$T_s \sim N\nu_c^{-1} = \frac{e^{\nu_c d/v_g}}{p\nu_c}. \tag{45}$$

Note that Eq.42 reduces to Eq.45 in the limit $p \to 0$, $\nu \to \infty$ and $v_g \ll v_s$.

	Budding Yeast (I)	mammalian (II)	*Xenopus* extracts(III)
ν_r	(0.42)0.12 min^{-1}	(10.5)2.7 min^{-1}	(0.66)1.2 min^{-1}
ν_c	(0.48)0.24 min^{-1}	((1.56)3.48 min^{-1}	(1.08)7.2 min^{-1}
v_g	1.7 μm min^{-1}	12.8 μm min^{-1}	12.3 μm min^{-1}
v_s	2.7 μm min^{-1}	14.1 μm min^{-1}	15.3 μm min^{-1}
R	2μm	20μm	500μm

TABLE I. Experimental values of microtubule kinetics in the mitotic phase. The values in parantheses are interphase values, prior to the cell entering mitosis, for Yeast[21], mammalian[15] and *Xenopus* extracts[22]. The cell radii given are only rough estimates. For theoretical and numerical analysis, we used $v_g = 2.0$ and $v_s = 3.0$ μm min^{-1} for I, and $v_g = 12.0$ and $v_s = 14.0$ μm min^{-1} for II and III. The experimental data for different cell sizes are summarized in [15].

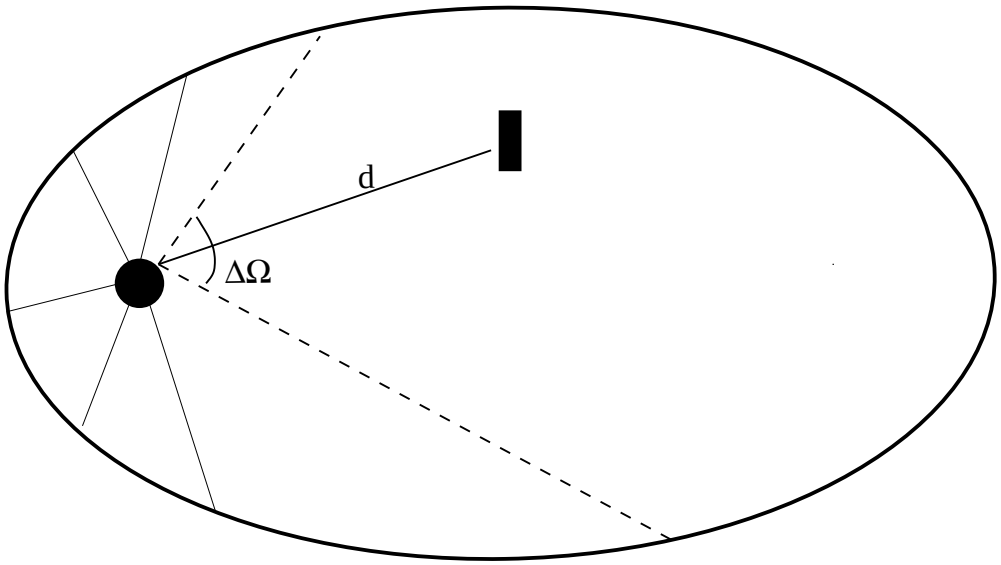

FIG. 1. A schematic illustration of the geometry of our model is shown here. Microtubules nucleate from nucleating sites on the centrosome, and search for a stationary target at a distance d. $\Delta\Omega$ is the solid angle of the 'search cone' for a certain nucleating site depicted in the picture. The search is curtailed by the cell boundary. The search cones of neighbouring nucleating sites may overlap (not shown here), which accelerates the process by 'parallel' search.

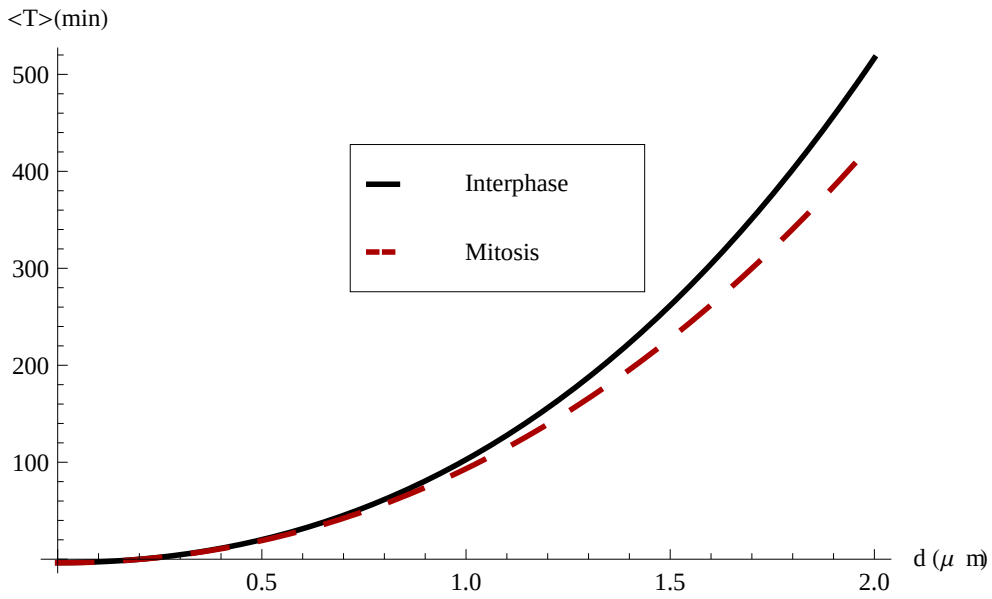

FIG. 2. The mean time of capture (in minutes) of a single chromosome in budding yeast, by microtubules from a single nucleating site, for various target distance d is shown here. The thick black like corresponds to interphase values of ν_r and ν_c. We assume the nuclear radius to be $R = 2\mu m$. The other parameters are $v_d = 3\mu$m min^{-1}, $v_g = 2\mu$m min^{-1}, $\nu = 0.1$min^{-1} and $\nu_c' = 10\nu_c$.

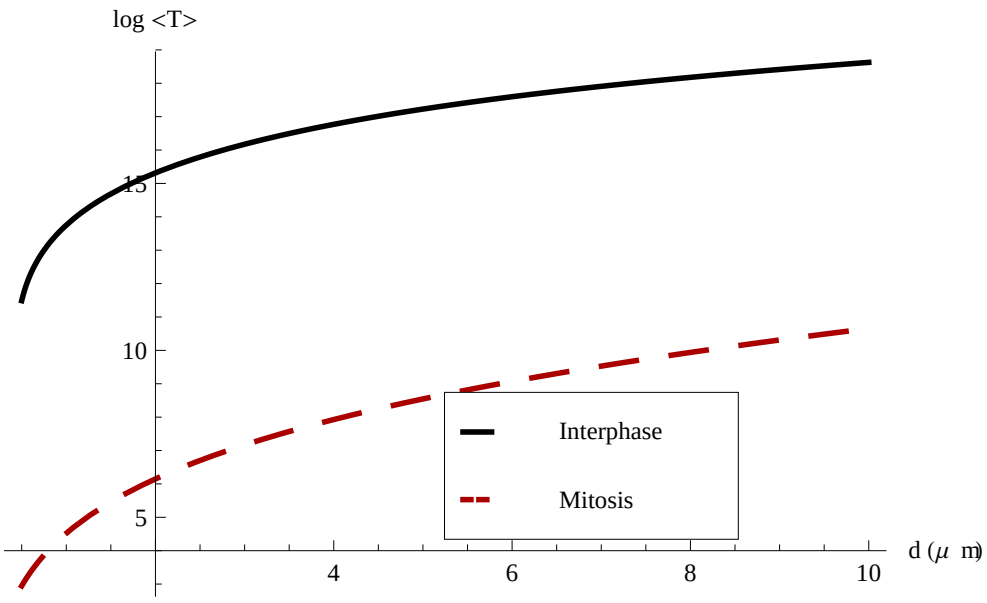

FIG. 3. Similar to the previous figure, but for mammalian cells. The cell radius is taken as $R = 20\mu$m. The other parameters are $v_d = 14\mu$m min^{-1}, $v_g = 12\mu$m min^{-1}, $\nu = 0.1$min^{-1} and $\nu_c' = 10\nu_c$.

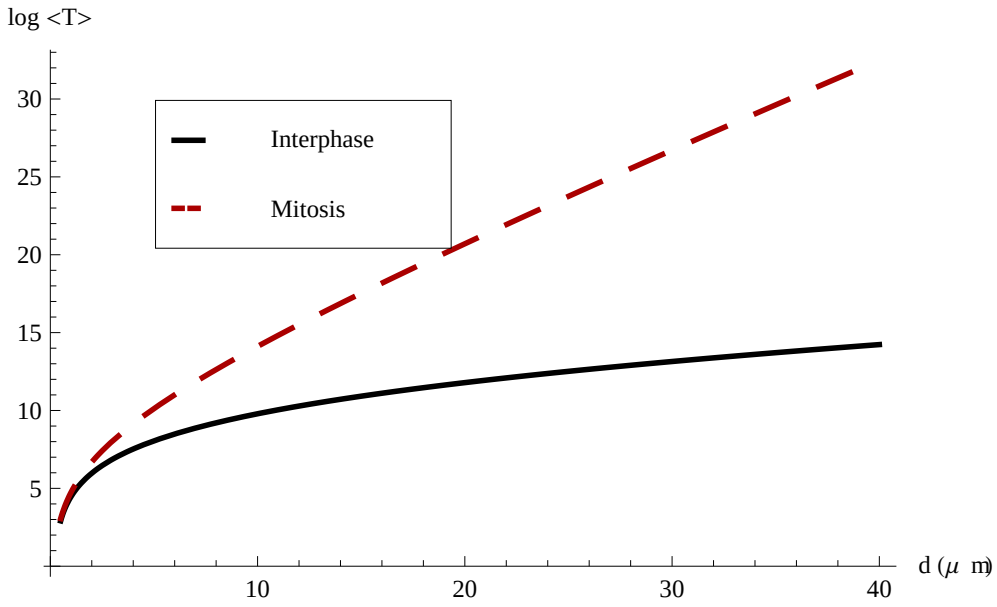

FIG. 4. Similar to the previous figures, but for *Xenopus* oocyte cells. The cell radius is taken as $R = 500\mu$m. The other parameters are $v_d = 15\mu$m min^{-1}, $v_g = 12\mu$m min^{-1}, $\nu = 0.1$min^{-1} and $\nu_c' = 10\nu_c$. Note that, unlike the previous figures, mitosis values appear to increase the search time compared to interphase, which suggests that the random search and capture mechanism might be inefficient in large cells.

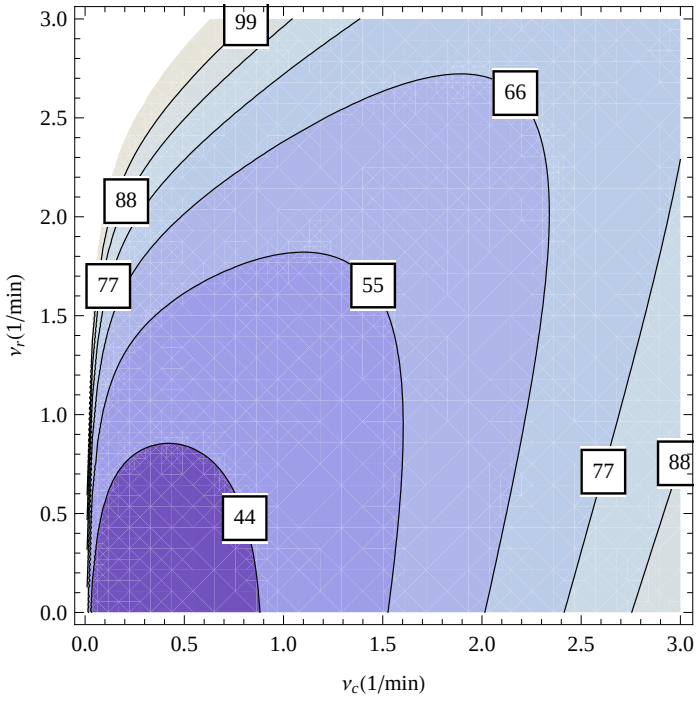

A.

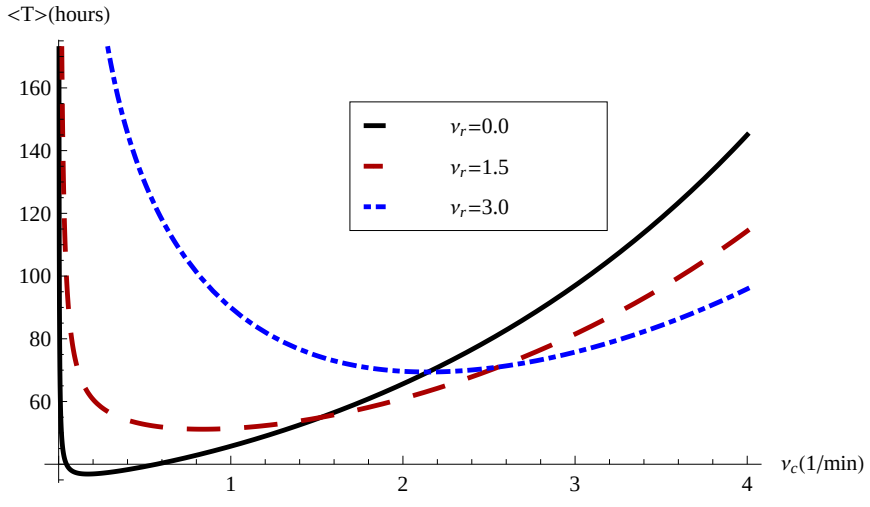

B.

FIG. 5. A. Contour plot for the mean search time (expressed in hours) of a single chromosome at $d = 6\mu$m, by a single nucleating site, in a mammalian cell with radius $R = 20\mu$ m. B. Cross-sections of the same plot at three values of ν_r. The parameters are $v_d = 14\mu$m min^{-1}, $v_g = 12\mu$m min^{-1}, $\nu = 0.1$min^{-1} and $\nu_c' = 10\nu_c$.

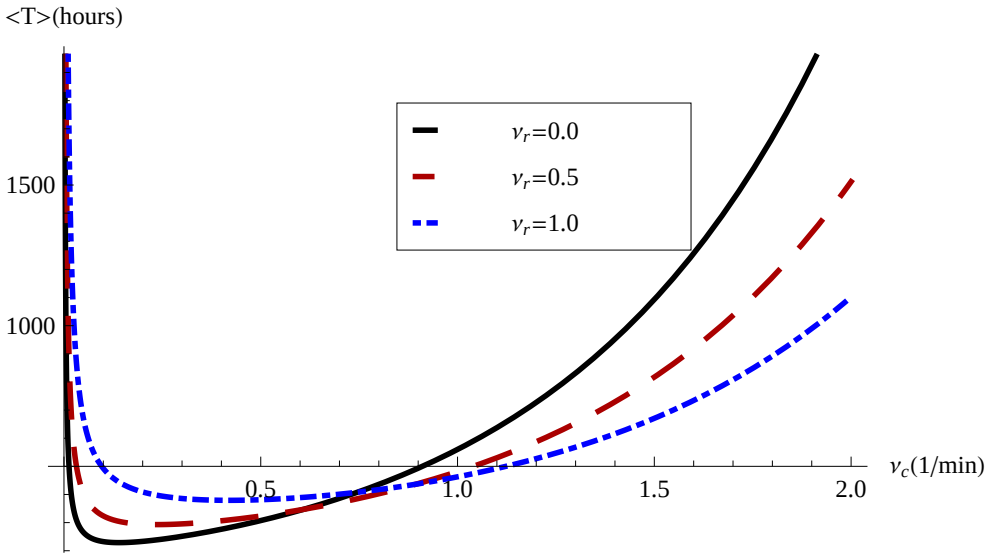

FIG. 6. The mean time of search for a target close to the boundary, at $d = 20\mu$m, in a cell of radius $R = 20\mu$m for three different ν_r. The other parameters are chosen as $v_s = 12\mu$m min^{-1}, $v_g = 10\mu$m min^{-1}, $\nu = 1$min^{-1} and $\nu_c' = 10\nu_c$. Note that slightly larger values of ν_r produce a more robust minimum as a function of ν_c, at the cost of a small increase in time.

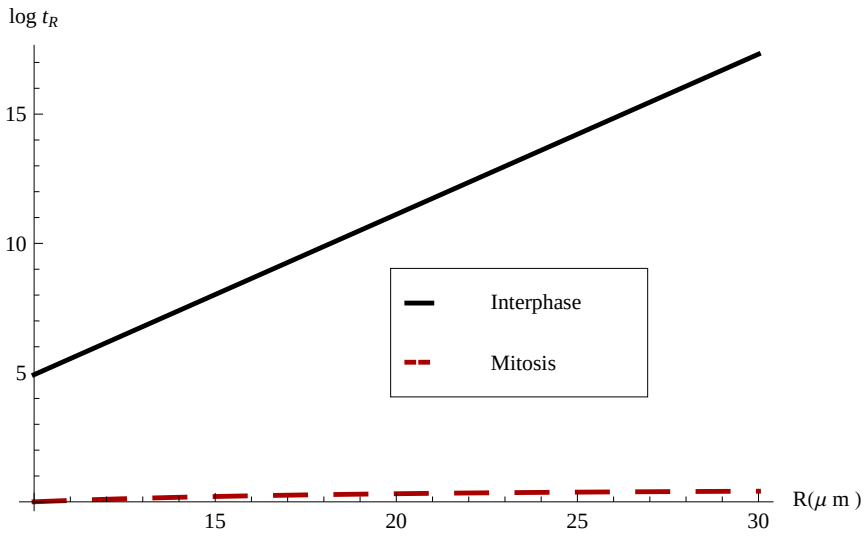

A.

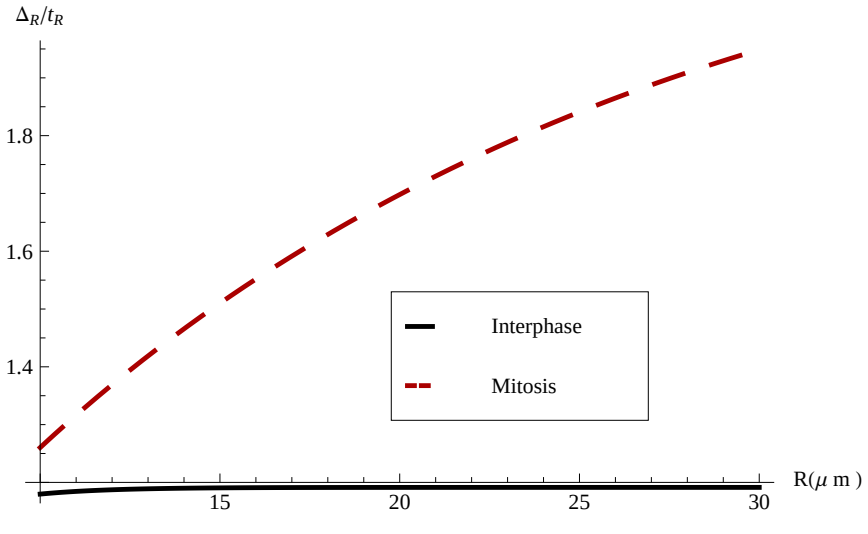

B.

FIG. 7. A. The mean lifetime t_R, defined as the mean lifetime of microtubules nucleating in directions away from the target (Eq.30), is plotted as a function of the cell radius R for interphase and mitotic parameter values. The lifetime in interphase is larger by several orders of magnitude.The parameter values are chosen as in Fig.4. B. The relative fluctuation in the lifetime, defined as the ratio of standard deviation Δ_R to the mean t_R, as a function of R, for the same set of parameter values. Fluctuations in the mitotic phase are larger than in interphase, signaling increased dynamicity of the microtubules.